

Microspectrophotometry of Nitric Oxide-Dependent Changes in Hemoglobin in Single Red Blood Cells Incubated with Stimulated Macrophages¹

Kazuhiro Tsujita,² Takuo Shiraishi, and Katsuko Kakinuma³

Biophotonics Information Laboratories, Yamagata Advanced Technology Research Center, Matsuei 2-2-1, Yamagata 990

Received for publication, December 27, 1996

A highly sensitive microspectrophotometer was developed to measure spectral changes of oxyhemoglobin (oxy Hb) in single red blood cells (RBC) incubated with stimulated macrophages as a model of nitric oxide (NO)-dependent cytotoxicity. Our microspectrophotometer, using a modified acousto-optic tunable filter (AOTF) and a 2-dimensional CCD array, allows fast spectrophotometric data acquisition. Human RBC treated with various concentrations of NO showed spectral changes due to the conversion of oxy Hb to methemoglobin (met Hb), in which the change in absorption differences at α (557-590 nm) and β (542-525 nm) bands showed a linear relationship with the concentration of NO up to 100 μ M. In contrast to highly diffusible NO, nitrite ions (NO_2^-) seem to enter RBC very slowly, resulting in negligible formation of met Hb in the presence of 5 mM glucose even during a prolonged incubation period. RBC were incubated with murine macrophages with and without lipopolysaccharide (LPS) in the presence of glucose for 24 and 40 h and subjected to the microspectrophotometric assay. The RBC incubated with LPS-stimulated macrophages showed significant changes in the spectrum due to NO-dependent conversion of oxy Hb to met Hb, which corresponded to the spectral changes of RBC treated with a several times higher concentration of NO than that in the culture medium. The trapping efficiency was calculated from the amounts of the NO released from macrophages and of the met Hb formed in the RBC, which gave a high efficiency (43%). The results suggest that RBC trap NO directly by cell-cell interaction with macrophages. This spectrophotometric system is available for use with just a few drops of samples to study NO-specific cytotoxicity as a model of RBC without the use of any chemical reagent, in parallel with microscopic observations on changes of the cellular morphology under physiological conditions, such as membrane damage leading to hemolysis, adherence, and phagocytosis.

Key words: acousto-optic tunable filter, macrophage, microspectrophotometry, nitric oxide, red blood cells.

Nitric oxide (NO) plays a role in a number of physiological and pathological processes (1-5). Nitric oxide in the blood is well maintained at a steady-state level of the order of micromolar by the dynamic balance between the continuous supply of NO by endothelial NO synthesis and the rapid scavenging of NO by oxy Hb in red blood cells (RBC) (4-7). Nitric oxide in the blood rapidly diffuses into RBC and reacts with oxy Hb to form met Hb, which is immediately reduced to deoxy Hb by active met Hb reductase in RBC, resulting in a very low residual concentration of NO (a few μ M in plasma) (8). Nevertheless, several studies have shown that macrophage-mediated cytotoxicity is linked to the release of large amounts of NO (10 to 100 μ M) by a

metabolic pathway that involves oxidation of L-arginine by the induced enzyme NO synthase (iNOS), in response to certain microbes or microbial products, such as bacterial lipopolysaccharides (LPS) and inflammatory cytokines (9, 10).

In the present investigation, we developed a highly sensitive microspectrophotometer using an acousto-optic tunable filter (AOTF) (11) and a 2-dimensional CCD array to measure the spectral changes in RBC due to NO-dependent conversion of oxy Hb to met Hb by stimulated macrophages. To measure the cytotoxicity of cellularly produced NO, it is desirable to avoid the use of externally added chemical reagents. This microspectrophotometric method can be used to monitor NO-dependent cytotoxicity as a model of RBC without the use of any chemical reagent, in parallel with examination of the cellular morphology under physiological conditions. By this technique, we observed NO-dependent conversion of oxy Hb to met Hb in the spectrum of RBC incubated with stimulated macrophages. From the absorption changes, the RBC incubated with stimulated macrophages trapped a several times

¹ This study was presented at Keio University International Symposium for Life Sciences and Medicine-1996 Conference on Oxygen Homeostasis and Its Dynamics on Dec. 8-13 1996, Tokyo.

² Present address: Fuji Photo Film Co., Ltd. Technology Development Center, Miyandai.

³ To whom correspondence should be addressed.

Abbreviations: AOTF, acousto-optic tunable filter; RBC, red blood cells.

higher concentration of NO than that in the culture medium measured by the Griess reaction method (12 a, b). The results are discussed with respect to the high trapping efficiency and the cell-cell interaction of RBC with stimulated macrophages under the culture conditions.

MATERIALS AND METHODS

AOTF-Based Microspectrophotometric System—A schematic diagram of our newly developed microspectrophotometric system is shown in Fig. 1A. The use of an acousto-optic tunable filter (AOTF) (11) and a 2-dimensional CCD array (CS8310, Tokyo Electric Industry) allows fast spectrophotometric data acquisition (13, 14). The white light image at the image plane of the microscope (TMD 300, Nikon) is filtered out by the AOTF, and then detected by a 2-dimensional CCD array. An image processor (DVS3000, Hamamatsu Photonics) is employed for electronic signal processing including integration, offset and

filtering. Absorption spectra are obtained in the range of 400–650 nm with 166 increments at 1.5 nm intervals. For spectroscopic imaging of biological samples over a wide range of visible wavelengths, we modified a commercial AOTF device (M-IM100, Brimrose), the schematic diagram of which is shown in Fig. 1B. The AOTF unit consists of a Gran-Taylor Prism, a TeO₂ crystal, a broadband polarizing beam splitter and relay lenses. The diffracted optical beam at the selected wavelength transmits through the beam splitter and is detected at the image plane 1 for spectrophotometry, while the undiffracted beam is reflected by the beam splitter and detected at image plane 2 as the object image. This modified AOTF unit offers several improved features: (1) extended wavelength range of 400 to 650 nm for practical use (the original AOTF unit covered a limited range of 550±100 nm), (2) improved optical efficiency (as much as 2.5 times at 500 nm), (3) simultaneous monitoring of the object image, (4) tracking of the sample areas for the location shifted during the wave-

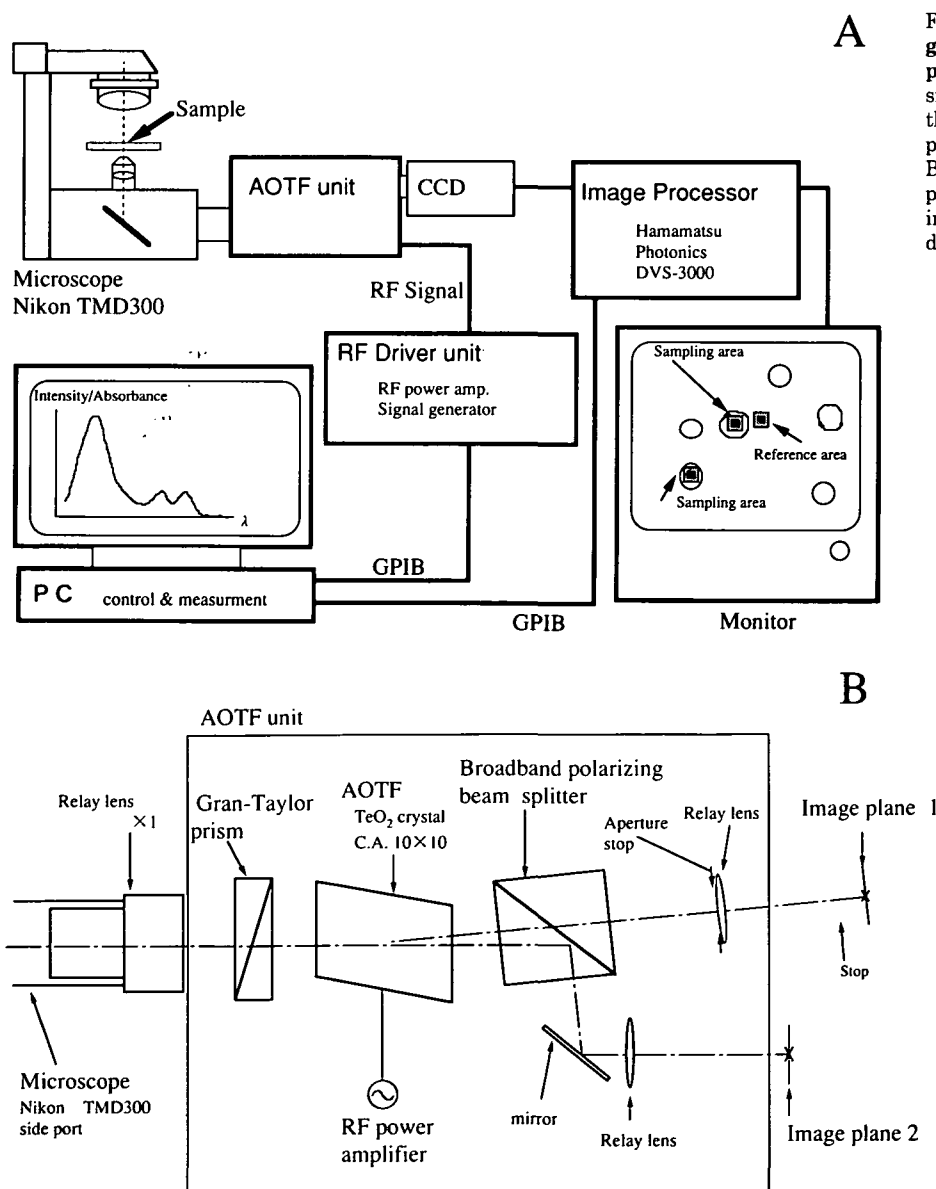


Fig. 1. A and B: Schematic block diagram of the AOTF-based microspectrophotometric system. A: This system consists of an AOTF unit (Fig. 1B) mounted at the side port of a microscope, an image processor, PC controller and a RF drive unit. B: The AOTF unit consists of a Gran-Taylor prism, a TeO₂ crystal, a broadband polarizing beam splitter and a relay lens. For details, see the text.

length-tuning, and (5) elimination of artifacts in the filtered image.

Microspectrophotometry—This system was used to measure spectra of RBC. The spectrophotometric measurement was carried out using a sampling area ($4 \times 4 \mu\text{m}^2$) for single RBC and an adjacent extracellular area as a reference, both of which were selected directly from the CRT screening in the image. The resolution of the sample image was limited to 6 by 6 pixels by the CCD camera and the number of sampling areas was varied in the range of 2 to 5 depending on the samples, all of which were identical in size. The data acquisition time was approximately 90 s.

Cell Preparations—Fresh RBC were collected from 20 ml of human venous blood, which was diluted 10-fold with Krebs Ringer phosphate buffer (KRP: 125 mM NaCl, 5.0 mM KCl, 1.2 mM MgCl_2 , and 20 mM phosphate buffer, pH 7.4) containing 5 mM glucose for microspectrophotometry. Macrophages were collected from peritoneal exudates of CD-1 mice four days after injecting thioglycollate into the peritoneal cavity according to the method previously reported (15).

Microspectrophotometry of Red Blood Cells (RBC)—(1) **Spectrophotometry on oxy Hb and CO Hb**: This microspectrophotometric system was tested on RBC in the absence and presence of CO to examine whether it could detect a small difference in the absorption spectra of oxy Hb and CO Hb. For oxy Hb, an aliquot of RBC was placed on a slide glass, covered with glass and shielded from evaporation, and then spectrometry was performed on a limited number (5 cells) of individual RBC. For CO Hb, 0.5 ml of the same diluted RBC was exposed to 50% CO in air, and an aliquot was then placed on a slide glass to measure the spectrum of CO Hb in individual RBC as described above. In all experiments, the spectra of five individual RBC were averaged.

To examine the photometric linearity, the hemolyzed venous blood was diluted with KRP buffer to heme concentrations of 0, 0.23, 0.46, 0.70, 0.93, and 1.16 mM, and an aliquot of silicon oil was dropped into each sample, which was placed in a hemocytometer (optical path: 100 μm). The spectrophotometry was conducted on sample areas of oxy Hb solutions with an adjacent area(s) containing the oil as the reference.

(2) **RBC Spectra in NO**: KRP buffer containing 5 mM glucose was deoxygenated in an air-tight tube by bubbling with N_2 gas, and then continuously bubbled with NO gas (99.7% pure) for 30 min to obtain 3 mM NO solution (16). An aliquot of the 3 mM NO solution was added to deoxygenated KRP buffer containing 5 mM glucose in an air-tight tube to make various concentrations of NO solution (30 to 300 μM) under N_2 gas flow, then 1/100 volume of RBC was injected with a microsyringe. The absorption spectra of the NO-treated RBC were measured using this microspectrophotometric system.

(3) **Effects of NO_2^- and glucose**: To examine the effects of nitrite ion (NO_2^-) on RBC absorption spectra, an aliquot of various concentrations of sodium nitrite (300 μM –3 mM) was added to RBC in KRP buffer in the presence and absence of 5 mM glucose. The spectral changes in RBC were measured for 3 h at various time intervals.

Microspectrophotometry on NO-Trapping RBC—Macrophages obtained as described above were suspended at a concentration of 8×10^5 cells per ml of the RPMI-1640

culture medium, and an aliquot (200 μl) was placed in each of 96 wells of microtiter plates and preincubated for 1.5 h at 37°C in air containing 5% CO_2 . The macrophage suspension was mixed with 10 $\mu\text{g}/\text{ml}$ of LPS and 84 U/ml of INF- γ as stimulators (15). An equal volume of the culture medium was added instead of the stimulators to other macrophages as resting cells. To both the macrophage suspensions in the microtiter plates for stimulated and resting cells, an aliquot of RBC was added to give a final concentration of 8×10^6 cells per ml. All the macrophage suspensions containing 5 mM glucose were incubated at 37°C for 24 and 40 h without shaking. The microspectrophotometry on RBC in these macrophage suspensions was carried out at various time intervals (0–40 h).

Assay of NO Production by Macrophages—In parallel experiments, the macrophage suspension was placed in other 96-well microtiter plates and incubated with and without the same stimulators in the presence of 5 mM glucose as described above, except for no addition of RBC, for the assay of NO by the Griess reaction method (12 a, b).

Reagents— NaNO_2 , sulfanilamide and *N*-(1-naphthyl)-ethylenediamine dihydrochloride (NED) were obtained from Wako Pure Chemical Industries, Tokyo. Interferon- γ (INF- γ) and lipopolysaccharide (LPS) were obtained from Sigma Chemical, St. Louis. Thioglycollate medium and culture medium (RPMI-1640) were obtained from Kanto Chemical, Tokyo, and Gibco BRL, NY, respectively. NO gas (99.7% pure) and CO gas (99.95% pure) were obtained from Sumitomo Seika Chemicals, Tokyo.

RESULTS AND DISCUSSION

Examination of the Microspectrophotometric System—This AOTF-based microspectrophotometric system could measure small spectral changes such as the absorption difference between oxy Hb and CO Hb with a limited number of RBC (1–5 cells) as shown in Fig. 2: the peaks shifted from 418 to 424 nm in the γ band, from 574 to 568 nm in the α band in accordance with characteristics of CO Hb (17). In addition, this system was able to measure

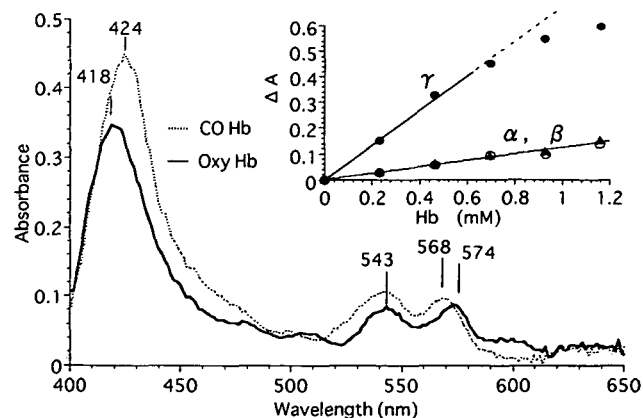


Fig. 2. Spectrophotometry of hemoglobin in red blood cells (RBC) and hemolyzed blood. RBC were treated with and without CO, and were subjected to microspectrophotometry. Solid line: oxy Hb, dotted line: CO Hb. Inset: Absorption spectra of oxy Hb in various concentrations of hemolyzed blood were measured using this system, and the absorbances at the α , β , and γ bands were plotted against the concentration of oxy Hb. For details, see the text.

absorption spectral changes in deoxy hemoglobin (deoxy Hb) under anaerobic conditions (data not shown). The absorption maxima at the α (574 nm), β (543 nm), and γ (418 nm) bands were measured with various concentrations of oxy Hb in hemolyzed blood according to the methods described above. The inset of Fig. 2 shows linearity of the absorbance at either the α or β band up to 1.2 mM oxy Hb, but at γ band only up to 0.46 mM oxy Hb. In addition, the absorbance at the γ band was 19% lower than that of the ordinary spectrum, due to the AOTF-unit, which had an optimal wavelength range from 500 to 600 nm. From these results, optical absorption maxima at the α and β bands were mainly used for evaluation of oxy Hb and met Hb, and the peak at the γ band was measured for characterization of the spectral shift throughout the present microspectrophotometry.

We examined the effect of NO on the absorption spectra of RBC at various concentrations as shown in Fig. 3. The α , β , and γ absorption bands of oxy Hb in RBC (Fig. 3, A) were shifted slightly from 575, 542, and 417 nm to 576, 539, and 416 nm in the presence of 30 μ M NO (Fig. 3, B). In the presence of 70 μ M NO, the absorption maximum at the γ band changed markedly from 417 to 413 nm, while the absorption maxima at the α and β bands shifted slightly from 575 to 578 nm and from 542 to 539 nm, respectively, though the absorbances decreased markedly (Fig. 3, C). The presence of 300 μ M NO resulted in disappearance of the absorption maxima at the α and β bands, and a marked shift of the absorption maximum at the γ band, by about 10 nm toward short wavelength (Fig. 3, D). The difference spectra of these spectral changes (the inset in Fig. 4) reflected the conversion of oxy Hb to met Hb, in good agreement with the difference spectra previously reported (18), i.e., absorption bands at 542 and 577 nm, and isosbestic points at 525 and 590 nm. The spectral changes in the α and β bands were expressed as the absorption differences between 577 and 590 nm and between 542 and 525 nm, respectively, which were plotted against the concentration of NO as shown in Fig. 4. The absorption differences at the

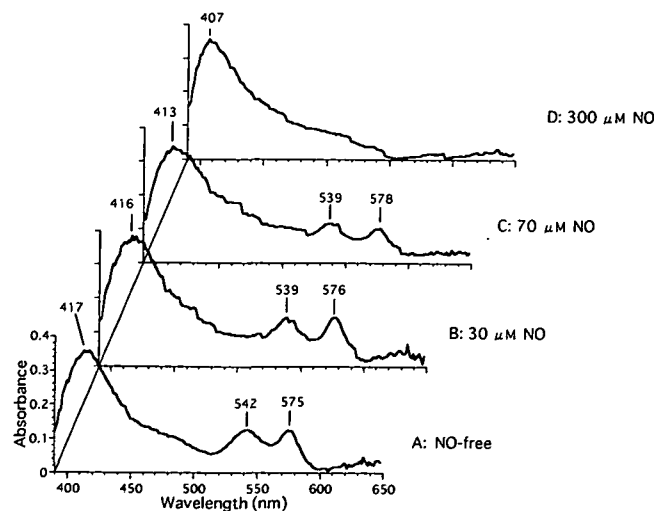


Fig. 3. Absorption spectra of RBC treated with various concentrations of NO. RBC were treated with 0 (A), 30 (B), 70 (C), and 300 (D) μ M NO, and subjected to microspectrophotometry. For details, see the text.

α and β bands showed a linear relation to the concentration of NO up to 100 μ M. A large deviation, however, was found at higher concentration (300 μ M NO), at which the intracellular hemoglobin was denatured (Fig. 3, D), some of the RBC showed Heinz bodies in the membranes (data not shown) and the number of RBC decreased markedly.

Since NO changes rapidly to NO_2^- in aqueous medium (12 a, b), the effect of NO_2^- on RBC was examined for comparison with the effect of NO with respect to met Hb formation in RBC: 300 μ M NO_2^- was added in RBC suspension in KRP buffer in the presence and absence of 5 mM glucose and the mixture was incubated at 37°C. The results are illustrated in Fig. 5, showing the time course of the absorption change at 540 nm in those RBC. In the

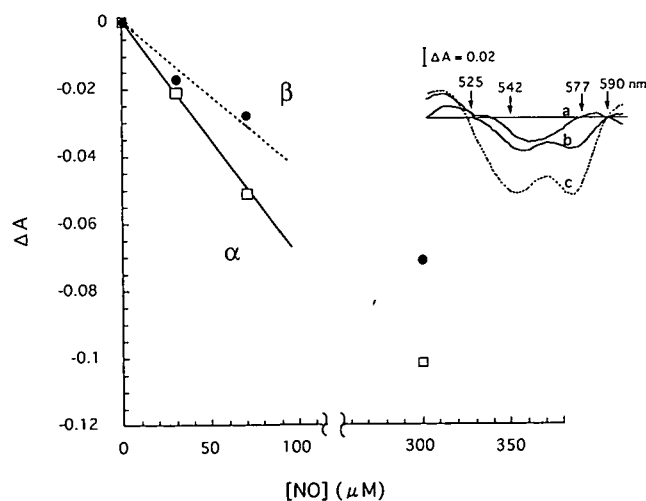


Fig. 4. Spectral changes of RBC treated with various concentrations of NO. From Fig. 3, the spectral changes of RBC with 30 (a), 70 (b), and 300 (c) μ M NO were recorded against the spectrum of NO-free RBC as a reference (base line) to obtain the difference spectra (Inset). The spectral changes in the α and β bands were measured as the absorption differences (ΔA) between 577 and 590 nm and between 542 and 525 nm, respectively, which were then plotted against the concentration of NO.

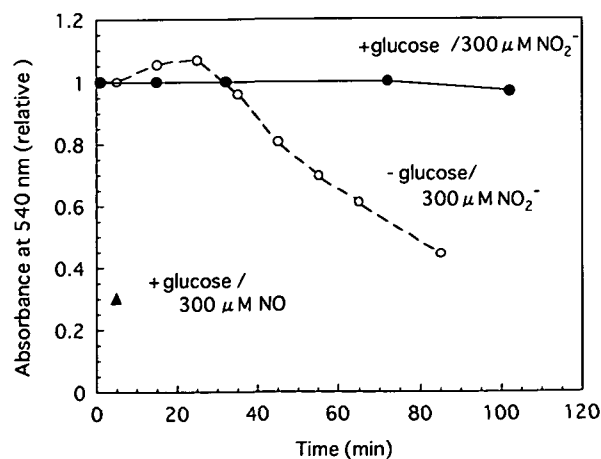


Fig. 5. Effect of NO_2^- on RBC in the presence and absence of glucose. RBC were incubated with 300 μ M NO_2^- in the presence and absence of 5 mM glucose (closed and open circles, respectively), and with 300 μ M NO in the presence of 5 mM glucose (triangle).

presence of glucose, no change in the absorbance was observed even after incubation for 100 min with NO_2^- (Fig. 5) and very little change was seen after three hours (data not shown). In the absence of glucose, the absorbance decreased gradually in the presence of $300 \mu\text{M}$ NO_2^- . In contrast, a rapid change in the spectrum occurred in the RBC treated with $300 \mu\text{M}$ NO in the presence of the same concentration of glucose, showing that NO permeates into RBC very quickly compared with NO_2^- , and thereby the intracellular hemoglobin is quickly oxidized by NO. NO_2^- ($300 \mu\text{M}$) seems to diffuse into RBC slowly due to its negative charge, as seen in the case of superoxide anion (19). From the results of Figs. 4 and 5, the microspectrophotometry on RBC was carried out with cultured cells in the presence of glucose as described below.

Microspectrophotometry on RBC Incubated with Stimulated Macrophages—A microscopic image of the macrophages incubated with RBC for 40 h in the presence of LPS and $\text{INF-}\gamma$ is shown in Fig. 6. RBC (diameter about $8 \mu\text{m}$) adhered to mature macrophages (diameter $40\text{--}45 \mu\text{m}$), so-called rosette formation (A1 and A2 in Fig. 6), because the adhesive reaction occurs in these macrophages after stimulation with LPS and $\text{INF-}\gamma$. RBC showed no adhesion to unstimulated macrophages, or monocytic cells (diameter $15\text{--}20 \mu\text{m}$) (B and C in Fig. 6). The present report deals mainly with the spectra of RBC which did not adhere to macrophages as illustrated in the inset of Fig. 6, though the hemoglobin spectrum of the adhered RBC was also measured as described later.

Absorption spectra of the RBC incubated with stimulated and resting macrophages for 0, 24, and 40 h are shown in Fig. 7, A and B, respectively. The absorption spectrum at 0 time was typical of oxy Hb, while RBC incubated with stimulated macrophages for 24 h showed a marked change in the spectrum; the γ band shifted 10 nm toward shorter wavelength and the β band showed a marked decrease in the absorbance. Further incubation for 40 h resulted in greater spectral changes; the disappearance of the α and β bands and the appearance of a new band around 500 nm,

and a marked shift of the γ band, which are characteristics of met Hb.

From Fig. 7A, the spectral changes of RBC incubated with stimulated macrophages were measured as the absorption differences between 577 and 590 nm and between 542 and 525 nm, at α and β bands, respectively, and were plotted against the incubation time as shown in Fig. 8. Both absorption differences showed a proportionality to the incubation time. The incubation for 24 h caused absorption changes of 0.05 and 0.037 at the α and β bands, respectively, which corresponded to the spectral changes of RBC treated with $70 \mu\text{M}$ NO (Fig. 4), three times as much as that measured by the Griess reaction ($23 \mu\text{M}$ NO) (12 a, b).

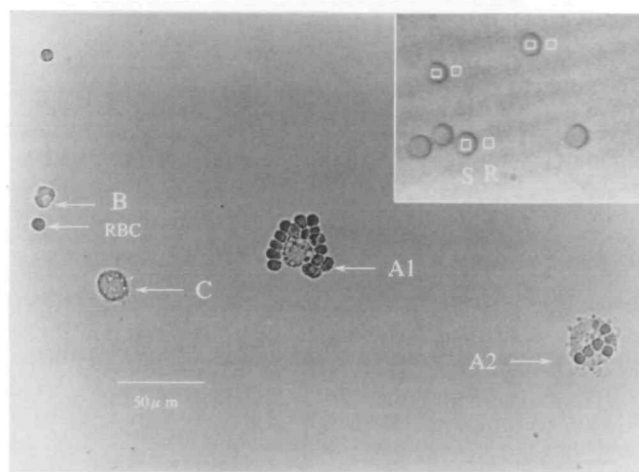


Fig. 6. Microscopic image of RBC incubated with macrophages. Macrophages incubated with RBC for 40 h with LPS and $\text{INF-}\gamma$. RBC adhered to the surface of matured macrophages (A1 and A2). Unstimulated macrophages (C), or monocytic cells (B) showed no adhesion to RBC. Inset: Microspectrophotometry of RBC incubated with stimulated macrophages was carried out with non-adhered RBC as shown by squares; a sampling area (S) for hemoglobin spectrum and a neighboring area (extracellular medium) for reference (R).

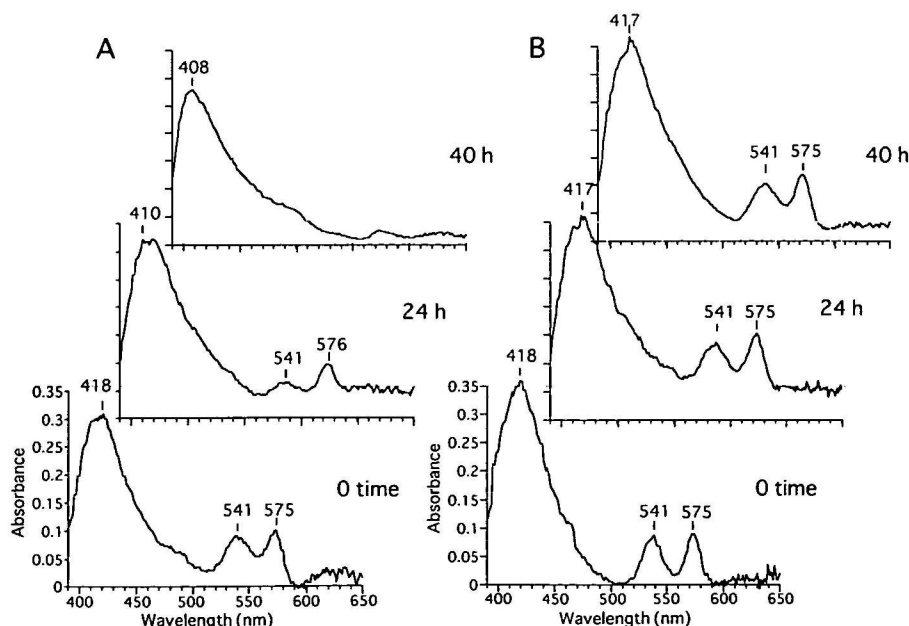


Fig. 7. Absorption spectra of RBC incubated with stimulated (A) and resting (B) macrophages. Macrophages were mixed with LPS and $\text{INF-}\gamma$ for stimulation and with the same volume of buffer for the control resting state, then RBC were placed on them and incubated for 40 h. The absorption spectra of RBC were measured at 0, 24, and 40 h.

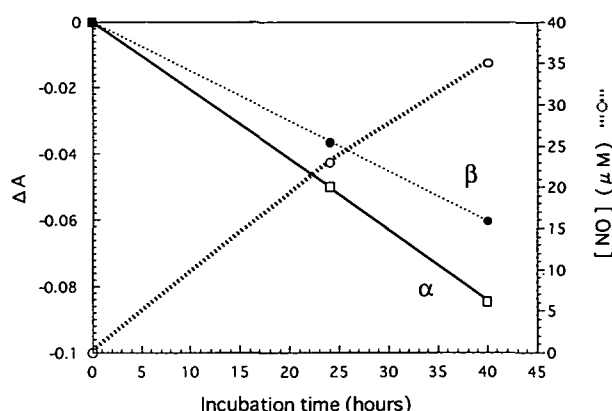


Fig. 8. Absorption changes of RBC incubated with stimulated macrophages and NO production. From the spectra of RBC incubated with stimulated macrophages (Fig. 7), the absorption differences (ΔA) between 577 and 590 nm and between 542 and 525 nm, at the α and β bands (open squares and closed circles) were plotted against incubation time (reference at 0 time). The concentration of NO produced by stimulated macrophages was measured by the Griess reaction method (open circles and broken line).

In addition, this microscopic image revealed time-dependent hemolysis of RBC: about 50% decrease in the number of RBC at 40 h as compared to that of resting macrophages. We conducted spectrophotometry on the RBC adhered to macrophages (A1 in Fig. 6), which exhibited also a complete conversion of oxy Hb to met Hb (data not shown), very similar to those of Fig. 3, D. Prior to hemolysis, macrophage-adhered RBC showed complete loss of oxy Hb, and some were ingested by macrophages. It is well known that stimulated macrophages generate superoxide anion, which is converted to hydrogen peroxide (20). Nitric oxide reacts rapidly with superoxide anion in aqueous solution, yielding peroxynitrite (21). Thus, the effects of superoxide dismutase and catalase were examined on the RBC incubated with stimulated macrophages. Neither superoxide nor hydrogen peroxide could explain such a marked conversion of oxy Hb into met Hb (data not shown). The superoxide generating-NADPH oxidase in phagocytes is a constitutive enzyme system which responds immediately to foreign materials to generate superoxide intensively for relatively short periods, a few to 30 min depending on the stimulators (20). In contrast to the NADPH oxidase system, the NO-generating enzyme system in macrophages is induced gradually after addition of bacterial materials such as LPS and generates NO for a long period; 24 to 40 h, as shown in Fig. 8. The two stages of O_2^- and NO generation by macrophages do not overlap, so that NO may scarcely react with O_2^- . In addition, in the former stage of O_2^- generation, met Hb reductase is still active (19), whereas in the latter stage, stimulated macrophages generate a large amount of NO which may inhibit met Hb reductase (5), leading to the significant change in the RBC spectrum, probably due to NO-dependent (O_2^- -independent) conversion of oxy Hb to met Hb.

The trapping efficiency [$\eta(\text{NO})$] of RBC was calculated from the data obtained by both the spectrophotometry and Griess reaction method as follows.

The total amount of NO produced by stimulated macro-

phages per well (200 μl) for 40 h (Fig. 8) was estimated to be

$$35 \times 10^{-6} \text{ (mol/liter)} \times 200 \times 10^{-6} \text{ (liter)} \\ = 7.0 \times 10^{-9} \text{ (mol)}$$

The total oxy Hb of RBC in the culture medium (1.6×10^6 RBC/well) which was completely converted to met Hb in 40 h (Fig. 7A), is calculated to be

$$21.8 \times 10^{-3} \text{ (mol/liter)} \times 86.1 \times 10^{-15} \text{ (liter)} \times 1.6 \times 10^6 \\ = 3.0 \times 10^{-9} \text{ (mol)}$$

where the concentration of oxy Hb in RBC is 21.8×10^{-3} (mol/liter) (17) and the volume of a single RBC is 86.1×10^{-15} (liter) (22). Thus, the trapping efficiency is calculated as follows, assuming that oxy Hb reacts with NO in the 1:1 ratio to form an equivalent amount of met Hb;

$$\eta(\text{NO}) \\ = [3.0 \times 10^{-9} \text{ (mol)} / 7.0 \times 10^{-9} \text{ (mol)}] \times 100 = 43(\%)$$

As compared with the met Hb formation by macrophages, the RBC treated with NO solution showed 100% conversion of the oxy Hb to met Hb in the presence of 300 μM NO.

The high efficiency suggests that RBC trap a local, high concentration of NO produced *in situ* by stimulated macrophages, since the spectral changes of RBC corresponded to those of RBC treated with a three to six times higher concentration of NO than that in the culture medium. The reactivity of NO with RBC seems to be a complex function of its diffusibility, its half life in aqueous medium, the membrane permeability, and the culture conditions (23). The culture medium contained RBC and macrophages in a ratio of 10:1 to get a high trapping efficiency by direct cell-cell interaction. As regards NO-dependent cytotoxicity, a localized high concentration of NO produced *in situ* by a cell or tissue is likely to be more important than that in the reaction medium. Recently, imaging of endogenous NO produced *in vitro* and *in vivo* has been achieved using chemiluminescence (24, 25) and ESR (26). This microspectrophotometer with AOTF, which allows fast spectrophotometry, could be available in the future for *ex vivo* monitoring of NO-dependent spectral changes in RBC in a vein or in an inflammatory lesion.

We thank Prof. Takashi Yonetani, Department of Biochemistry, University of Pennsylvania, for his valuable suggestions and a critical reading of the manuscript. We thank Dr. Teruo Kirikae and Prof. Masayasu Nakano, Department of Microbiology, Jichi Medical School, for their kind guidance in the preparation of macrophages and the assay of NO production, and Dr. Tetsuhiko Yoshimura, Institute for Life Support Technology, Yamagata Technopolis Foundation, for his helpful suggestions.

REFERENCES

1. Furchgott, R.F. and Zawadzki, J.V. (1980) The obligatory role of endothelial cells in the relaxation of arterial smooth muscle by acetylcholine. *Nature* **288**, 373-376
2. Moncada, S., Palmer, R.M.J., and Higgs, E.A. (1991) Nitric oxide: physiology, pathophysiology, and pharmacology. *Pharmacol. Rev.* **43**, 109-142
3. Feldman, P.L., Griffith, O.W., and Stuehr, D.J. (1993) The surprising life of nitric oxide. *Chem. Eng. News* **71**, 26-38
4. Ignarro, L.J., Buga, G.M., Wood, K.S., Byrns, R.E., and Chaudhuri, G. (1987) Endothelium-derived relaxing factor produced and released from artery and vein is nitric oxide. *Proc. Natl. Acad. Sci. USA* **84**, 9265-9269

5. Kosaka, H., Uozumi, M., and Tyuma, I. (1989) The interaction between nitrogen oxides and hemoglobin and endothelium-derived relaxing factor. *Free Radical Biol. Med.* **7**, 653-658
6. Kon, K., Maeda, N., and Shiga, T. (1977) Effect of nitric oxide on the oxygen transport of human erythrocytes. *J. Toxicol. Environ. Health* **2**, 1109-1113
7. Wennmalm, A., Lanne, B., and Petersson, A.-S. (1990) Detection of endothelial-derived relaxing factor in human plasma in the basal state and following ischemia using electron paramagnetic resonance spectrometry. *Anal. Biochem.* **187**, 359-363
8. Feelisch, M. (1993) Biotransformation to nitric oxide of organic nitrates in comparison to other nitrovasodilators. *Eur. Heart J.* **14** (Suppl.), 123-132
9. Stuehr, D.J. and Marletta, M.A. (1985) Mammalian nitrate biosynthesis: Mouse macrophages produce nitrite and nitrate in response to *Escherichia coli* lipopolysaccharide. *Proc. Natl. Acad. Sci. USA* **82**, 7738-7742
10. Nathan, C. (1992) Nitric oxide as a secretory product of mammalian cells. *FASEB J.* **6**, 3051-3064
11. Chang, I.C. (1981) Acousto-optic tunable filters. *Opt. Eng.* **20**, 824-829
12. a) Schmidt, H.H.H.W. and Kelm, M. (1996) in *Methods in Nitric Oxide Research* (Feelisch, M. and Stamler, J.S., eds.) pp. 491-497, John Wiley & Sons, New York
b) Ignarro, L.J., Fukuto, J.M., Griscavage, J.M., Rogers, N.E., and Byrns, R.E. (1993) Oxidation of nitric oxide in aqueous solution to nitrite but not nitrate: Comparison with enzymatically formed nitric oxide from L-arginine. *Proc. Natl. Acad. Sci. USA* **90**, 8103-8107
13. Kurtz, I., Dwelle, R., and Katzka, P. (1987) Rapid scanning fluorescence spectroscopy using an acousto-optic tunable filter. *Rev. Sci. Instrum.* **58**, 1996-2003
14. Tran, C.D. and Simianu, V. (1992) Multiwavelength thermal lens spectrophotometer based on an acousto-optic tunable filter. *Anal. Chem.* **64**, 1419-1425
15. Kirikae, F., Kirikae, T., Qureshi, N., Takayama, K., Morrison, D.C., and Nakano, M. (1995) CD14 is not involved in *Rhodobacter sphaeroides* diphosphoryl lipid a inhibition of tumor necrosis factor alpha and nitric oxide induction by taxol in murine macrophages. *Infect. Immun.* **63**, 486-497
16. Tracey, W.R., Linden, J., Peach, M.J., and Johns, R.A. (1990) Comparison of spectrophotometric and biological assays for nitric oxide (NO) and endothelium-derived relaxing factor (EDRF): Nonspecificity of the diazotization reaction for NO and failure to detect EDRF. *J. Pharmacol. Exp. Ther.* **252**, 922-928
17. Antonini, E. and Brunori, M. (1971) *Hemoglobin and Myoglobin in Their Reactions with Ligands*, North-Holland, Amsterdam, London
18. Feelisch, M., Kubitzek, D., and Werringloer, J. (1996) in *Methods in Nitric Oxide Research* (Feelisch, M. and Stamler, J.S., eds.) pp. 455-477, John Wiley & Sons, New York
19. Tomoda, A., Suzuki, H., Fukuhara, Y., Ueda, Y., Niho, K., Yoneyama, Y., and Kakinuma, K. (1984) Involvement of active oxygens released by activated leukocytes in hemolytic mechanism of G6PD deficient red cells. *Acta Haematol. Jpn.* **47**, 189-194
20. Rossi, F. (1986) The O₂⁻-forming NADPH oxidase of the phagocytes: nature, mechanisms of activation and function. *Biochim. Biophys. Acta* **853**, 65-89
21. Stamler, J.S., Singel, D.J., and Loscalzo, J. (1992) Biochemistry of nitric oxide and its redox-activated forms. *Science* **258**, 1898-1902
22. Westerman, M.P., Pierce, L.E., and Jensen, W.N. (1961) A direct method for the quantitative measurement of red cell dimensions. *J. Lab. Clin. Med.* **57**, 819-824
23. Vanderkooi, J.M., Wright, W.W., and Erecinska, M. (1994) Nitric oxide diffusion coefficients in solutions, proteins and membranes determined by phosphorescence. *Biochim. Biophys. Acta* **1207**, 249-254
24. Leone, A.M., Furst, V.W., Foxwell, N.A., Cellek, S., and Moncada, S. (1996) Visualisation of nitric oxide generated by activated murine macrophages. *Biochem. Biophys. Res. Commun.* **221**, 37-41
25. Kikuchi, K., Nagano, T., Hayakawa, H., Hirata, Y., and Hirobe, M. (1993) Real time measurement of nitric oxide produced *ex vivo* by luminol-H₂O₂ chemiluminescence method. *J. Biol. Chem.* **268**, 23106-23110
26. Yoshimura, T., Yokoyama, H., Fujii, S., Takayama, F., Oikawa, K., and Kamada, H. (1996) *In vivo* EPR detection and imaging of endogenous nitric oxide in lipopolysaccharide-treated mice. *Nature, Biotech.* **14**, 992-993